Journal of Geophysical Research: Planets

Supporting Information for

Full-field modeling of heat transfer in asteroid regolith 2: Effects of porosity

Andrew J. Ryan[1], Daniel Pino-Muñoz[2], Marc Bernacki[2], Marco Delbo[3], Naoya Sakatani[4], Jens Biele[5], Joshua P. Emery[6], Benjamin Rozitis[7]

[1]Lunar and Planetary Laboratory, University of Arizona, Tucson, AZ, USA; [2]Centre de mise en forme des matériaux (CEMEF), Mines ParisTech, PSL Research University, Sophia Antipolis, France; [3]Observatoire de la Côte d'Azur, CNRS-Lagrange, Université Côte d'Azur, Nice, France; [4]Rikkyo University, Tokyo, Japan; [5]German Aerospace Center (DLR), Köln, Germany; [6]Department of Astronomy and Planetary Sciences, Northern Arizona University, Flagstaff, AZ, USA. [7]School of Physical Sciences, The Open University, Milton Keynes, UK.

Contents of this file

Introduction

Here we include supplemental figures and tables that provide the reader more details on our method of model validation, experimental data recalibration, and resulting values from our numerical simulations. The filenames given in Tables S1–S3 and S6 correspond to the vtk geometry files available in an external data archive (Ryan, 2022; https://doi.org/10.5281/zenodo.5839026).

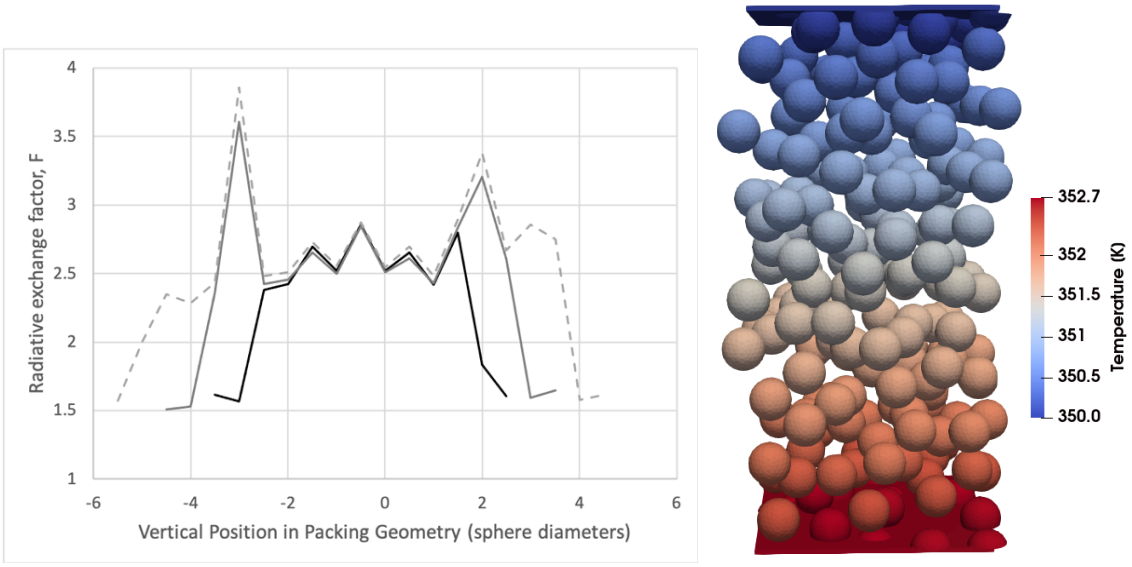

Figure S1. Example of variations in local radiative exchange factor, F, within a random sequential packing of spheres. Increasing the thickness of the packing changes the values of F near the edge plates but does not significantly affect F near the center of the geometry (<5% change). The packing on the right is the thickest of the three shown in the plot on the left, colorized by the steady-state temperature solution.

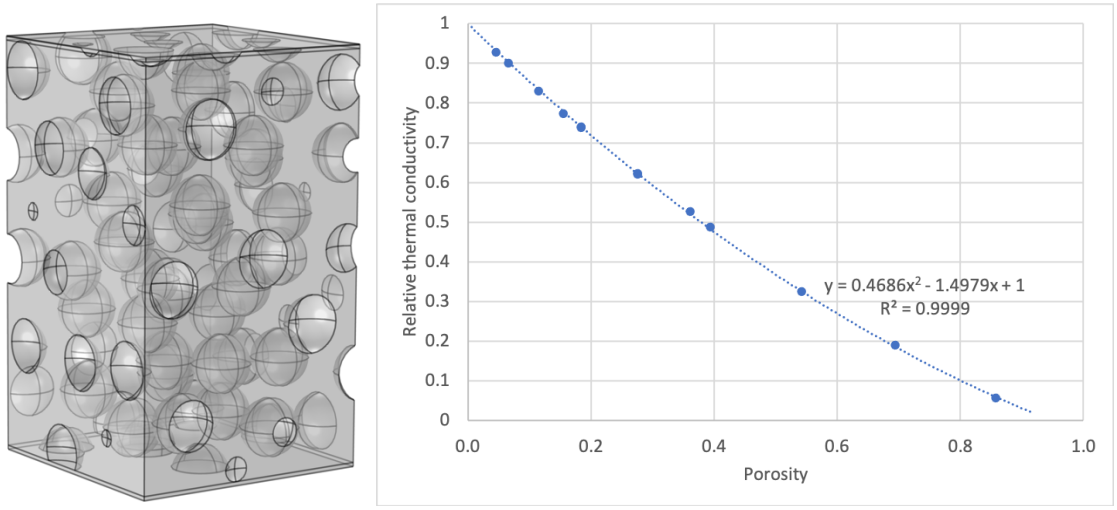

Figure S2. Vesicular "swiss cheese" rock model geometry (left) used to estimate the relationship between porosity and relative thermal conductivity in porous volcanic rock (right).

Table S1. Calculated porosity and radiative exchange factor values for random packings. BPCA=Ballistic particle-to-cluster accumulation; RSP= Random sequential packing; BCCA=Ballistic cluster-to-cluster accumulation; Ringl = Ringl et al. (2012) method; ODR = optimized dropping and rolling (Hitti and Bernacki, 2013). Filenames in **bold** are packings shown in Figure 1. The filename in *italics* is shown in Figure S1.

Packing style and filename	Porosity			F		
	Mean	Max	Min	Mean	Max	Min
BPCA						
bpca_5_8_v4b_res_02000	0.595	0.603	0.583	1.516	1.537	1.486
bpca_4.5_10_v1_res_01500	0.619	0.657	0.589	1.803	1.904	1.711
bpca_5_8_v3d_k30.0_res_03000	0.631	0.636	0.627	1.772	1.783	1.762
RSP						
rsp_5_7_166_res_01500	0.631	0.652	0.612	1.878	1.947	1.744
rsp_5_20-11_res_01800	0.644	0.662	0.629	2.031	2.160	1.900
rsp_5_7_160_k30.0_res_02500	0.648	0.664	0.617	1.963	2.029	1.922
rsp_4.5_9_150_res_01500	0.663	0.696	0.627	1.987	2.015	1.938
rsp_4.5_10_130_k30_res_02000	0.709	0.730	0.687	2.334	2.793	2.095
rsp_5_20-11_shrink045_res_01000	0.736	0.749	0.726	2.693	2.890	2.489
rsp_4.5_12_130_res_01500	0.753	0.782	0.715	2.682	3.168	2.450
rsp_4.5_14_130_k30.0_res_01400	0.779	0.813	0.742	2.817	3.382	2.407
rsp_5_14_150_res_01500	0.791	0.813	0.760	3.092	3.758	2.601
rsp_6_12_170_res_00500	0.822	0.848	0.810	3.618	3.741	3.396
BCCA						
bcca_4.5_8.0_128_2_k30_res_02400	0.674	0.701	0.647	2.165	2.522	1.973
bcca_5_6.4_128_2_res_01000	0.731	0.748	0.711	2.455	2.686	2.296
bcca_5_12_256_3_res_00500	0.747	0.798	0.692	2.676	2.911	2.561
bcca_5_12_256_4_res_01400	0.760	0.820	0.679	2.841	3.127	2.548
bcca_6_12_256_2gen_res_00700	0.790	0.816	0.777	3.393	3.884	2.886
bcca_6_12_256_2gen_v2_res_00400	0.810	0.848	0.765	3.789	4.476	3.438
Ringl						
ssgen_050_4_6_res_01400	0.578	0.582	0.574	1.492	1.553	1.430
ssgen_050_4_6_rough3_res_00500	0.687	0.710	0.656	2.093	2.146	1.994
ODR						
odr2_res_03000	0.456	0.464	0.445	1.279	1.330	1.206
odr4_k30.0_res_03000	0.470	0.480	0.455	1.257	1.295	1.213
odr3_res_01500	0.473	0.497	0.456	1.256	1.293	1.202

Table S2. Calculated porosity and radiative exchange factor values for regular (ordered) packings.

Packing style and filename	Porosity	F
Simple Cubic		
cubshrink_0499_long10_res_02500	0.496	1.224
cubshrink_0485_long10_res_03500	0.538	1.322
cubshrink_0475_long10_res_03500	0.566	1.414
cubshrink_046_long12_res_02500	0.606	1.552
cubshrink_044_long10_res_03200	0.655	1.782
cubshrink_040_long14_res_02500	0.741	2.424
cubshrink_035_long12_res_01100	0.826	3.505
Body-centered cubic		
cubCentre_long4_res_04000	0.337	0.990
cubCentre_048_long4_res_02400	0.404	1.067
cubCentre_044_long4_res_02200	0.542	1.339
cubCentre_040_long4_res_01400	0.657	1.797
cubCentre_035_long4_res_01600	0.771	2.660
Face-centered Cubic		
cubiqueFaceCentree_long4_res_02400	0.278	0.913
fccshrink_049_long4_res_02400.vtk	0.315	0.930
fccshrink_048_long4_res_02400.vtk	0.356	0.977
fccshrink_047_long4_res_02400.vtk	0.395	1.021
fccshrink_046_long4_res_02400.vtk	0.433	1.078
fccshrink_044_long4_res_02600.vtk	0.504	1.212
fccshrink_040_long4_res_01400.vtk	0.626	1.640
fccshrink_035_long4_res_00400.vtk	0.750	2.480

Table S3. Calculated porosity, radiative exchange factor, f_k, and $(1-\varphi)/\Lambda s$ for all simulations related to investigating the non-isothermality correction factor.

Packing type, porosity avg (max, min), and filenames	F			f_k	$(1-\varphi)/\Lambda s$
	mean	max	min		
BPCA, φ=0.623 (0.636, 0.627)					
bpca_5_8_v3d_k30.0_res_03000	1.772	1.783	1.762	1	1.214E-03
bpca_5_8_v3d_k6.0_res_02200	1.761	1.772	1.751	0.994	6.071E-03
bpca_5_8_v3d_k1.0_res_03000	1.696	1.708	1.685	0.957	3.646E-02
bpca_5_8_v3d_k0.6_res_02500	1.650	1.663	1.638	0.931	6.082E-02
bpca_5_8_v3d_k0.25_res_03000	1.516	1.531	1.502	0.855	1.463E-01
bpca_5_8_v3d_k0.1_res_02500	1.292	1.309	1.277	0.729	3.674E-01
bpca_5_8_v3d_k0.05_res_01800	1.092	1.107	1.076	0.616	7.392E-01
RSP, φ=0.648 (0.664, 0.617)					
rsp_5_7_160_k30.0_res_02500	1.963	2.029	1.922	1	1.158E-03
rsp_5_7_160_k5.0_res_02500	1.944	2.004	1.907	0.990	6.950E-03
rsp_5_7_160_k3.0_res_02000	1.930	1.985	1.895	0.983	1.159E-02
rsp_5_7_160_k0.6_res_02000	1.809	1.830	1.798	0.921	5.801E-02
rsp_5_7_160_k0.25_res_02000	1.649	1.666	1.629	0.840	1.395E-01
rsp_5_7_160_k0.1_res_02000	1.391	1.445	1.318	0.708	3.504E-01
rsp_5_7_160_k0.05_res_02000	1.169	1.244	1.066	0.595	7.046E-01
RSP, φ=0.709 (0.730, 0.687)					
rsp_4.5_10_130_k30_res_02000	2.334	2.793	2.095	1	9.603E-04
rsp_4.5_10_130_k1.0_res2000	2.230	2.639	2.010	0.956	2.885E-02
rsp_4.5_10_130_k0.6_res_01500	2.171	2.551	1.962	0.930	4.811E-02
rsp_4.5_10_130_k0.25_res_02000	2.005	2.309	1.826	0.859	1.151E-01
rsp_4.5_10_130_k0.1_res_01900	1.735	1.935	1.599	0.743	2.854E-01
rsp_4.5_10_130_k0.05_res2000	1.487	1.613	1.387	0.637	5.844E-01
RSP, φ=0.779 (0.813, 0.742)					
rsp_4.5_14_130_k30.0_res_01400	2.817	3.382	2.407	1	7.251E-04
rsp_4.5_14_130_k2.0_res_04000	2.771	3.304	2.379	0.984	1.088E-02
rsp_4.5_14_130_k1.0_res_01400	2.724	3.226	2.351	0.967	2.177E-02
rsp_4.5_14_130_k0.25_res_01900	2.500	2.858	2.209	0.888	8.724E-02
rsp_4.5_14_130_k0.1_res_02400	2.224	2.654	1.933	0.789	2.173E-01
rsp_4.5_14_130_k0.05_res_03400	1.975	2.498	1.635	0.701	4.358E-01
BCCA φ=0.674 (0.701, 0.647)					
bcca_4.5_8.0_128_2_k30_res_02400	2.165	2.522	1.973	1	1.073E-03
bcca_4.5_8.0_128_2_k1.5_res_02500	2.093	2.419	1.924	0.967	2.147E-02
bcca_4.5_8.0_128_2_k0.6_res_00600	1.999	2.287	1.841	0.923	5.372E-02

bcca_4.5_8.0_128_2_k0.25_res_04000	1.827	2.055	1.687	0.844	1.286E-01
bcca_4.5_8.0_128_2_k0.1_res_02900	1.549	1.700	1.430	0.715	3.209E-01
bcca_4.5_8.0_128_2_k0.05_res_03000	1.304	1.408	1.200	0.602	6.437E-01
bcca_4.5_8.0_128_2_k0.025_res_04000	1.085	1.163	0.990	0.501	1.293E+00
ODR, φ=0.470 (0.480, 0.455)					
odr4_k30.0_res_03000	1.257	1.295	1.213	1	1.748E-03
odr4_k6.0_res_02000	1.247	1.285	1.204	0.992	8.704E-03
odr4_k0.6_res_03000	1.153	1.184	1.116	0.917	8.762E-02
odr4_k0.25_res_03000	1.040	1.062	1.012	0.827	2.109E-01
odr4_k0.1_res_05700	0.855	0.869	0.839	0.680	5.256E-01
odr4_k0.05_res_04000	0.692	0.705	0.682	0.550	1.045E+00
odr4_k0.025_res_05700	0.542	0.554	0.532	0.431	2.100E+00

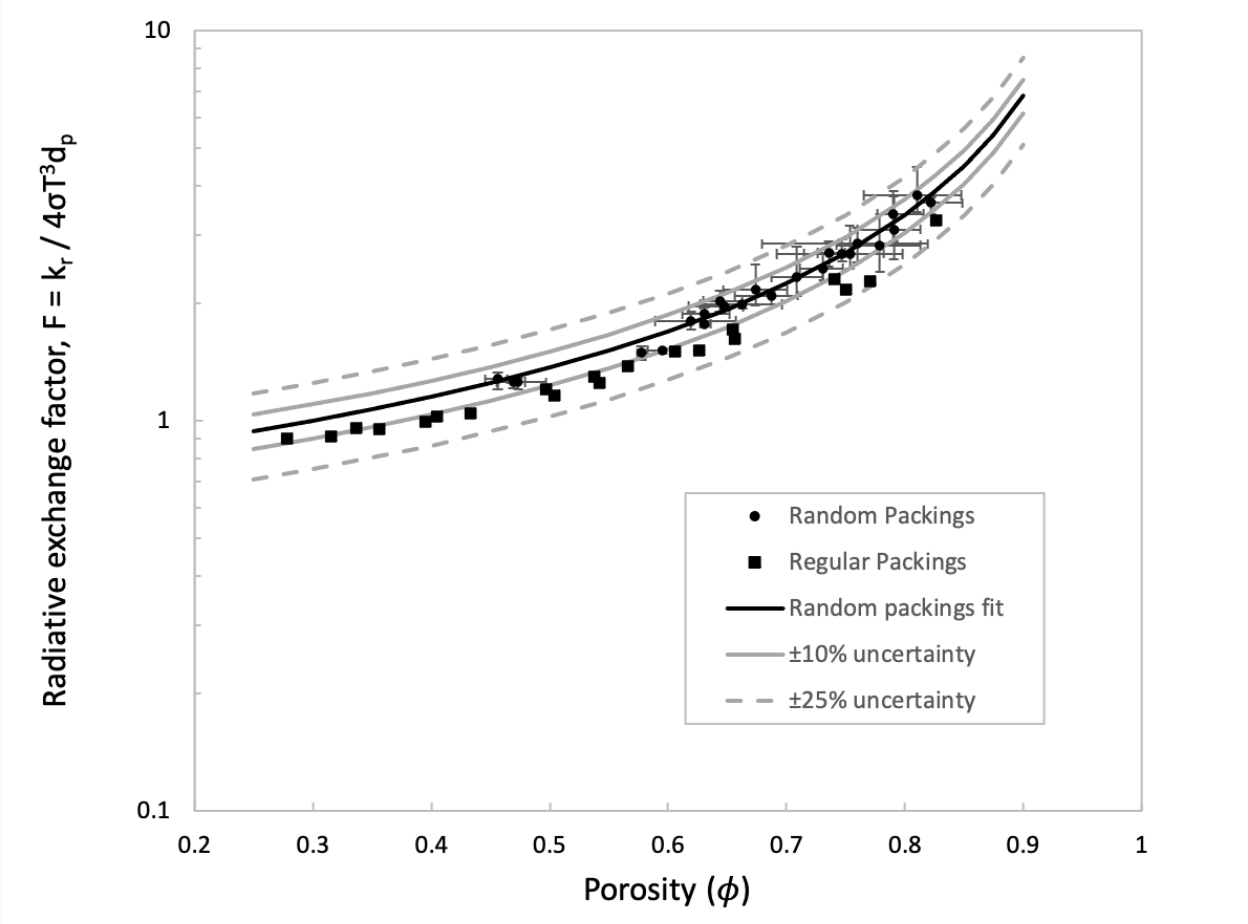

Figure S3. Trendline for random packing data with ±10% and ±25% uncertainty bounds shown.

Table S4. Full results of reanalysis of 710–1000 µm experimental data from Sakatani et al. (2018) using revised values for assumed macroporosity, particle size, emissivity, and material thermal conductivity as described in main text. Values in **bold** are the originally reported particle density and macroporosity values from Sakatani et al. (2018). Values in *italics* are measured values from water pycnometry. As a reminder, "porosity" here refers to the void fraction between particles, a.k.a. macroporosity, and is not to be confused with total bulk porosity.

Porosity (phi)	Assumed particle density	Micro-porosity	With changes only to assumed macroporosity and particle density			With all changes described in text		
			F	zeta	xi	F	zeta	xi
0.66	**2900**	0	0.831	0.680	0.683	0.859	0.842	0.918
0.636	*2693*	0.071	0.831	0.690	0.576	0.859	0.872	0.864
0.6	2450	0.16	0.831	0.726	0.451	0.859	0.918	0.779
0.55	2177.8	0.25	0.831	0.777	0.330	0.859	0.982	0.676
0.5	1960	0.32	0.831	0.831	0.248	0.859	1.050	0.590
0.45	1781.8	0.39	0.831	0.889	0.189	0.859	1.123	0.516

Table S5. Full results of reanalysis of 355–500 µm experimental data from Sakatani et al. (2018) using revised values for assumed macroporosity, particle size, emissivity, and material thermal conductivity as described in main text. Values in **bold** are the originally reported particle density and macroporosity values from Sakatani et al. (2018). Values in *italics* are measured values from water pycnometry. As a reminder, "porosity" here refers to the void fraction between particles, a.k.a. macroporosity, and is not to be confused with total bulk porosity.

Porosity (phi)	Assumed particle density	Micro-porosity	With changes only to assumed macroporosity and particle density			With all changes described in text		
			F	zeta	xi	F	zeta	xi
0.62	**2900**	0	1.136	0.966	0.327	1.162	1.206	0.440
0.609	*2838*	0.021	1.137	0.981	0.303	1.162	1.225	0.420
0.6	2775	0.043	1.137	0.993	0.285	1.162	1.240	0.410
0.55	2466.7	0.15	1.137	1.063	0.208	1.162	1.328	0.355
0.5	2220	0.23	1.137	1.137	0.155	1.162	1.420	0.310
0.45	2018.2	0.30	1.137	1.216	0.118	1.162	1.518	0.270

Table S6. Results for two sets of simulations where the spheres were roughened by adding spherical section craters to the sphere surfaces. Two packing geometries were used; the results presented for each include the original values (no roughness) and those that were obtained after the spheres were roughened with craters. Filename in bold is shown in Figure 2.

Designation and filename	Porosity			F		
	Mean	Max	Min	Mean	Max	Min
Rough results 1						
ssgen_050_4_6_res_01400 (no roughness)	0.578	0.582	0.574	1.492	1.553	1.430
ssgen_050_4_6_rough3_res_00500	0.603	0.608	0.597	1.485	1.554	1.416
Rough results 2						
ssgen_035_4_7_res_01300 (no roughness)	0.687	0.710	0.656	2.093	2.146	1.994
ssgen_035_4_7_rough3_res_00500	0.730	0.745	0.704	2.112	2.162	2.041